

Multi-ultraflatbands tunability and effect of spin-orbit coupling in twisted bilayer transition metal dichalcogenides

Zhen Zhan,¹ Yipei Zhang,¹ Guodong Yu,^{1,2} Francisco Guinea,³ José Ángel Silva-Guillén,^{1,*} and Shengjun Yuan^{1,†}

¹*Key Laboratory of Artificial Micro- and Nano-structures of Ministry of Education and School of Physics and Technology, Wuhan University, Wuhan 430072, China*

²*Institute for Molecules and Materials, Radboud University, Heijendaalseweg 135, NL-6525 AJ Nijmegen, The Netherlands*

³*Fundación IMDEA Nanociencia, C/Faraday 9, Campus Cantoblanco, 28049 Madrid, Spain*

Ultraflatbands that have been theoretically and experimentally detected in a bunch of van der Waals stacked materials show some peculiar properties, for instance, highly localized electronic states and enhanced electron-electron interactions. In this Letter, using an accurate *ab initio* tight-binding model, we study the formation and evolution of ultraflatbands in transition metal dichalcogenides (TMDCs) under low rotation angles. We find that, unlike in twisted bilayer graphene, ultraflatbands exist in TMDCs for almost any small twist angles and their wave function becomes more localized when the rotation angle decreases. Pressure and local deformation can tune the width of the flatbands, as well as their localization. Furthermore, we investigate the effect of spin-orbit coupling on the flatbands and discover spin/orbital/valley locking at the minimum of the conduction band at the K point of the Brillouin zone. The ultraflatbands found in TMDCs with a range of rotation angle below 7° , may provide an ideal platform to study strongly correlated states.

Introduction.—Stacked van der Waals layered systems provide an ideal platform to modulate the electronic properties of their parent materials via different degrees of freedom, for example, the rotation angle [1, 2]. One of the most interesting phenomenon in these twisted two-dimensional (2D) materials is the formation of flatbands. Recently, it has been discovered that, in the so-called magic-angle twisted bilayer graphene, a flatband forms near the Fermi level and strongly correlated states, for instance, a Mott insulating behavior and unconventional superconductivity, arise from such flatband [3, 4]. This generated an intensive investigation on this matter in order to identify bilayer systems that present this kind of electronic properties and that could be used as an ideal platform to study many-body interaction physics.[5–8]. Soon after, flatbands were also theoretically predicted and experimentally observed in transition metal dichalcogenides (TMDCs) [8–22].

The engineering of the quantum states of matter is an active area of the experimental and theoretical research on modern condensed matter physics. In two-dimensional crystals and van der Waals materials, such controllable engineering can be realized by means of the rotation angle, pressure, strain or local deformation.[23, 24] For instance, the modification of the magic angle value of twisted bilayer graphene has been realized by application of a uniaxial strain [25]. In fact, atomically thin 2D materials are particularly suited for strain engineering. For example, single-particle bound states can be created and confined by strain at the center of bubbles in monolayers of TMDCs [26]. A strain superlattice can lead to bands which describe a topological insulator[27]. As a designing parameter, the interlayer coupling can be tuned by variable local stackings to tailor the electronic properties of van der Waals materials [28–30]. How these

tuning parameters engineer the ultraflatbands and their novel properties of twisted bilayer TMDCs is still unclear.

In this Letter, we use an accurate *ab initio* tight-binding Hamiltonian[31, 32] to study the electronic properties of twisted bilayer MoS₂ (TBLM) and, in particular, the engineering of the emerging ultraflatbands at low rotation angles. We find that multiple energy-separated ultraflatbands are formed in rigidly twisted TMDCs with tiny twist angle. Furthermore, applying pressure can induce more flatbands and shift them towards the Fermi level, which indicates a tendency of the system to suffer a semiconductor-to-metal transition. More interestingly, the mechanical strain applied at some high-symmetry stackings can destroy or create ultraflatbands at the valence band (VB) edge and change the localization of the wave functions of these flatbands as well. In the presence of the strong spin-orbit coupling (SOC), the spin/valley/orbital locking is detected at the K point of the Brillouin zone (BZ) of the conduction band (CB) minimum in TBLM. That is different from the single-layer TMDCs case where the spin polarization is probed at the so-called Q point [33]. This property can be of interest for the implementation of these structures in novel valleytronics devices.

We construct the twisted bilayer TMDCs by starting from a 2H stacking and rotating the top layer with an angle θ with respect to the bottom layer around an atom site [32, 34]. The Moiré pattern has D_3 point group symmetry with the threefold rotation axis perpendicular to the TMDCs plane and three two-fold rotation axes in the TMDCs plane. As illustrated in Ref. 32, in the supercell we can distinguish three different high-symmetry stackings (AB, B^{S/S} and B^{Mo/Mo}). The band structure of monolayer transition metal dichalcogenides can be described by a tight-binding Hamiltonian consist-

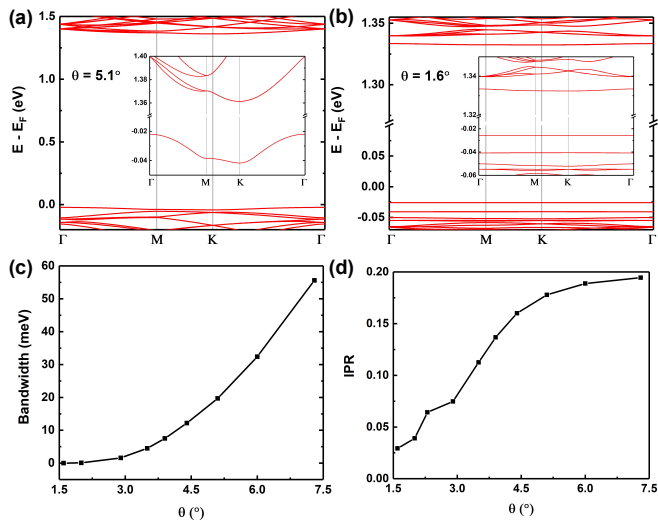


FIG. 1. The band structure of twisted bilayer MoS_2 with angle (a) $\theta = 5.1^\circ$ and (b) $\theta = 1.6^\circ$. Insets are the conduction and valence band edges. (c), (d) Variation of the bandwidth and the inverse participation ratio (IPR) changes with the rotation angle.

ing of eleven orbitals, the d orbitals from Mo and the p orbitals from the S. The generalization to the bilayer case (including the twisted bilayer system) is done by adding an interlayer hopping term of the p orbitals of the chalcogen between adjacent layers to a two single-layer Hamiltonian [31, 32, 35]. In this work we used an *ab initio* TB Hamiltonian which further improves the fitting of the band structure. [31] Tight-binding models are quite useful for the investigation of large-scale complicated systems and for the systematic study of local strain effect on the electronic properties of 2D materials.

Rotation angle.—Via exact diagonalization of the *ab initio* tight-binding Hamiltonian of the twisted bilayer MoS_2 , we carefully study the evolution of band structures under different rotation angle from $\theta = 7.3^\circ$ to $\theta = 1.6^\circ$, which are illustrated in Fig. 1. Recently, by using first-principles density functional theory (DFT), ultraflatbands have been discovered in TBLM with rotation angle $\theta = 5.1^\circ$ [9]. The shape of the ultraflatband in Fig. 1(a) is similar to that of the DFT result. When the rotation angle approaches 0° , for instance $\theta = 1.6^\circ$ (see Fig. 1(b)), multiple energy-separated ultraflatbands emerge at the valence band edge, which are localized at the $B^{S/S}$ region [10, 11]. Moreover, an ultraflatband forms at the conduction band edge and its wave function is localized at the $B^{\text{Mo/Mo}}$ region. These ultraflatbands resemble the quantized energy levels of bound states of a particle in a potential well, indicating that the electron suffers a strong and deep effective moiré potential [10, 11]. The ultraflatbands also occur at the valence band edge of twisted bilayer MoSe_2 , WS_2 and WSe_2 as well (see Sec. E of the Supplementary Information (SI) [36]), which is

consistent with a recent experimental result [12].

We define the bandwidth W as the energy difference between the Γ and K points in the valence band edge. To characterize the band flattening, we plot the evolution of bandwidths W with θ in Fig. 1(c). The bandwidth undergoes a drastic changes from 30 meV to nearly zero as the rotation angle decreases. There are two reasons that can explain the flattening of bands. i) The first is trivial, the growing size of the moiré unit cell shrinks the moiré Brillouin zone (MBZ). Since the MBZ is smaller than the original BZ, the energy bands simply fold into the MBZ and could cause the band flattening. ii) On the other hand, the evolution of the interlayer interaction due to the formation of a moiré structure can also cause band flattening while resulting in a non-trivial modulation of the electronic properties. It was discovered both theoretically and experimentally that in twisted bilayer systems, the electronic states of the flatbands are highly localized at the $B^{S/S}$ or $B^{\text{Mo/Mo}}$ high-symmetry stacking regions in the real space, trapped by the effective periodic moiré potential and forming networks analogous to arrays of quantum dots [9–11].

To compare the localization of wave functions in the TBLM, we calculate the inversion participation ratio (IPR), which in a tight-binding model with N orbitals is defined as [37]:

$$IPR = 1/(N \sum_{i=1}^N |a_i^\alpha|^4), \quad (1)$$

where a_i^α is the amplitude for the eigenstate α at the site i . The evolution of the IPR of the states at K in the VB edge is plotted in Fig. 1(d). As the rotation angle becomes smaller, the IPR decreases monotonically, showing an evidence of electron localization. This is a strong signal of a moiré-modulated electronic band structure instead of one caused by trivial band-folding. Therefore, we can conclude that the change of the interlayer interaction due to the change in the moiré structure is the reason behind the flattening of the bands.

Compression.—The possibility of modifying the ultraflatbands and their associated correlated physics in twisted bilayer TMDCs by the application of uniaxial compression is investigated. In Fig. 2(a) we can see that, for TBLM with $\theta = 2.0^\circ$, the ultraflatbands emerge in both CB and VB edges. Compression in the direction perpendicular to the bilayers is implemented in terms of $\sigma = 1 - (d'/d)$ where d' is the distance between repeating two monolayer units and d is the distance at zero compression. For simplicity, the effect of compression on the in-plane lattice parameters are ignored.

If we pull apart the layers (negative compression), the ultraflatbands near the CB and VB edges go deeper into the CB and VB, respectively and disappear, whereas the top VB ultraflatband is robust. More interestingly, as the positive compression increases, the layers come closer

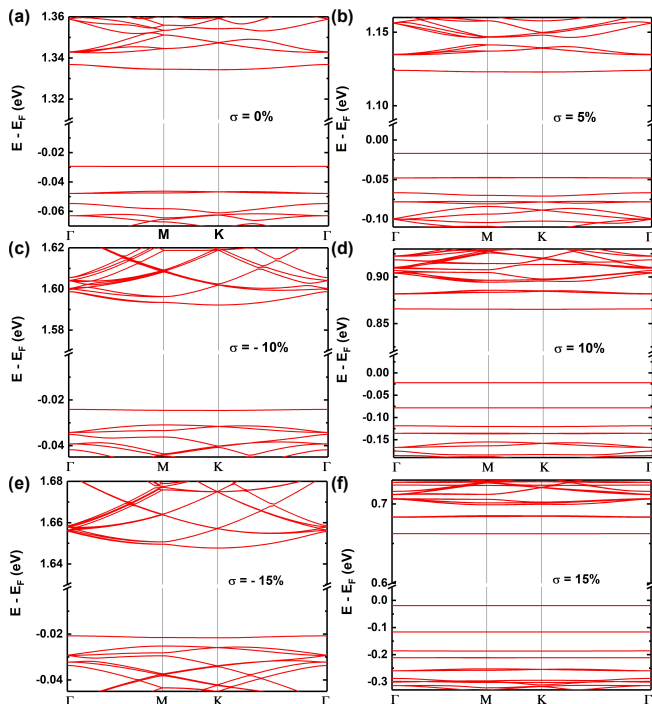


FIG. 2. The band structure of twisted bilayer MoS₂ with $\theta = 2.0^\circ$ under different vertical compression.

and the effective interlayer coupling strength increases, which creates more energy-separated ultraflatbands in both CB and VB edges. Such multiple energy-separated ultraflatbands is similar to the DFT result in Ref. 10. The compression has no effect on the localization of the ultraflatbands (see Sec. A of the SI[36]). Moreover, a progressive closure of the band gap is obtained as the compression increases, which indicates that a metallization of twisted TMDCs may occur at compression larger than 15%. Such metallization could be investigated in an experimental setup with the application of pressure on TBLM higher than 56 GPa [38].

Local deformation.—Specific strain textures can be produced in a system by applying an external strain, indenting with nanopillars patterned in a substrate or stacking one layer on another lattice-mismatched layer [39–43]. The structural deformation can have a significant influence on the electronic properties of such systems. For instance, spatially tailored pseudo-magnetic fields were detected in graphene-based devices[34, 43]. How will the local deformation affect the ultraflatbands in twisted bilayer TMDCs is still unclear. In this part, a Gaussian-type bubble with a radius $R = 2.6$ nm is created at a high-symmetry stacking region (AB or B^{S/S}) of the TBLM with $\theta = 2^\circ$. The in-plane separation between the high-symmetry stacking sites is 9 nm. The center of the bubble is located at either the AB or B^{S/S} site (see Fig. 3) and the maximum out-of-plane displacement, h_{max} , at AB and B^{S/S} is $0.05c$ and $0.2c$, respectively. The bubble

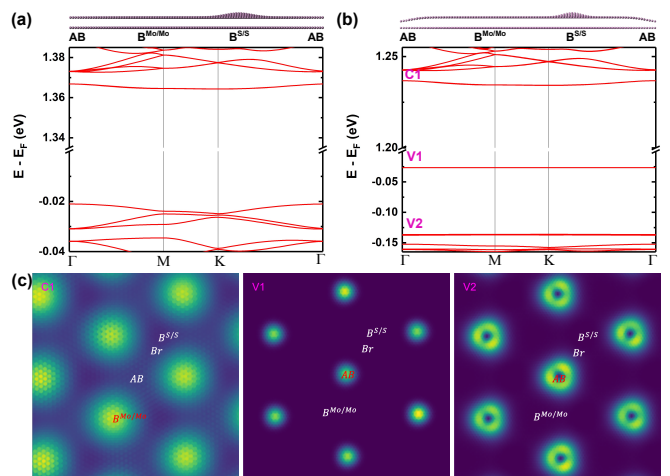


FIG. 3. The band structure of 2° twisted bilayer MoS₂ with local deformation at (a) the B^{S/S} region and (b) both the AB and B^{S/S} regions. The insets are the side view of the atomic model along the direction of the three high-symmetry stacking (AB, B^{Mo/Mo} and B^{S/S}). The local deformation is realized by implementing a Gaussian-type bubble at the B^{S/S} or AB regions and with the center located at the B^{S/S} or AB site, respectively. (c) The calculated local density of states mapping with energies of the CB and VB edges labeled in (b).

has a height-over-radius ratio $h_{max}/R = 0.04$, in which the in-plane lattice deformation can be neglected. We only concentrate on the interlayer coupling and, for simplicity, we will use the same in-plane hopping value that independently of the lattice deformation.

In Fig. 3(a), the multiple ultraflatbands that are localized at the B^{S/S} region are destroyed upon the formation of the bubble. When the interlayer distance increases inside the bubble, the interlayer interaction decreases, which kills the ultraflatband in the VB edge. After, we can generate a concave bubble with the same shape at the AB region (see inset of Fig. 3(b)). Interestingly, as seen in Fig. 3(b), multiple energy-separated ultraflatbands form again in the VB edges. When the height of the bubble increases, more ultraflatbands appear in the VB. Different from the moiré pattern without local deformation, as shown in Fig. 3(c), the new ultraflatband states are localized at the AB region. Differently, the local deformation in both AB and B^{S/S} regions have minor changes to the ultraflatband in the CB edge and its localization. All in all, the local deformation is remarkably efficient to tune the ultraflatband as well as its localization.

Spin-orbit coupling.—Transition metal dichalcogenides, in particular, single-layer TMDCs, have strong spin-orbit coupling (SOC) and broken inversion symmetry which lead to opposite spin polarization on different valleys. The locked spin and valley pseudospin gives rise to rich valley physics and makes TMDCs promising materials

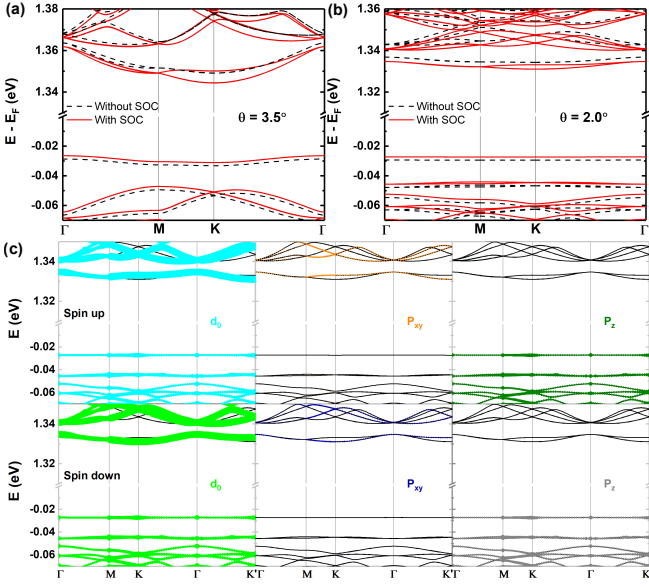


FIG. 4. The band structure of twisted bilayer MoS₂ with rotation angles (a) $\theta = 3.5^\circ$ and (b) $\theta = 2.0^\circ$. The red solid and black dashed lines are the band structure with and without spin-orbit coupling, respectively. (c) The band structure and orbital weight of 2° twisted bilayer MoS₂. The thickness of the bands represents the orbital weight with the d character ($d_2 = d_{x^2-y^2}, d_{xy}, d_1 = d_{xz}, d_{yz}, d_0 = d_{3z^2-r^2}$) refers to the Mo atom $4d$ orbitals and p character ($p_{xy} = p_x, p_y$) refers to S atom $2p$ orbitals. The orbital weight of d_2 and d_1 are not shown here. The sum orbital weight of d_0, p_{xy} and p_z is up to 97%.

for next generation optoelectronic applications. In the tight-binding model, the effect of SOC is well captured by doubling the orbitals and including an on site term $\sum_{\alpha} \lambda_{\alpha} \mathbf{L} \cdot \mathbf{S}$ in the Hamiltonian, where subscript α stands for the type of atom[31, 33].

In this section, we investigate the effect of SOC on the band structure of twisted bilayer MoS₂. The band structure with (red solid line) and without spin-orbit coupling (dashed black line) is shown in Fig 4(a) and (b) for $\theta = 3.5^\circ$ and $\theta = 2.0^\circ$, respectively. From these figures we observe that, upon rotation, as a consequence of breaking the out-of-plane mirror symmetry, spin degeneracies are lifted along the Γ -K-M path, but the time reversal invariant points Γ and M remain spin degenerate. Furthermore, opposite to the single-layer case, the effect of SOC is more significant in the conduction band for the twisted bilayer system. This is the opposite to what happens in a MoS₂ monolayer, where the effect of the spin-orbit interaction is negligible for the conduction band. In the monolayer, the conduction band edge, at the K point, has a $d_{3z^2-r^2}$ character[35]. For these states, $(\mathbf{L} \cdot \mathbf{S}) = 0$, and the effect of the spin-orbit requires processes of second order in perturbation theory[44]. The twisted system considered here has regions which resemble differ-

ent stacking configurations of MoS₂ bilayers, where the bands at the Q point in the Brillouin Zone can be below the states at the K point. Hence, the states at the Q point of MoS₂ have a contribution to the flat bands studied here, see Fig.[S4] in [36]. These states have a significant $S p_x, p_y$ character, where the splitting due to the spin-orbit coupling is a first order process. Our results suggest that, in order to understand the conduction band of twisted MoS₂, a model based solely on the states at the K and K' points is insufficient.

Focusing on the conduction and valence band edges, we found that the ultraflatband at the valence band edge is doubly spin-degenerate in the whole BZ and, as shown in Fig. 4, there is no spin splitting at the VB edge. Meanwhile, at the conduction band edge, the K valley has the largest spin splitting and shrinks when the rotation angle decreases. This can be qualitatively understood in terms of the variation of the spin splitting at the Q point of the BZ in different high-symmetry stackings, that is, the SOC splitting is sensitive to the interlayer interaction (see Sec. D of the SI [36]).

We further calculate the orbital weight for the band structure of TBLM with $\theta = 2^\circ$. The ultraflatband at the valence band edge is mainly composed of d_0 and p_z orbitals and is indeed spin-degenerate. States at the bottom of the conduction band mainly consist of p_{xy} and d_0 orbitals, and the two in-equivalent valleys degree are spin-locked. That is, the spin up states at valley K are degenerate with spin down states at valley K', and vice-versa. That is different from the monolayer case where the Q point has the band splitting with a spin-polarization[33]. Note that the electronic state of the ultraflatband at the valence band is highly localized at the B^{S/S} position where the interlayer interaction is the strongest. Thus, the large composition of p_z orbital at valence band edge indicates a strong evidence of competition between the moiré interlayer interaction and the SOC. Therefore, we attribute the suppressed effect of SOC on the valence band as a consequence of a nearly restored in-plane inversion symmetry for bilayers with small twist angles, and also the modulation of moiré potential. We also pay attention to the evolution of orbital contribution for the conduction band edge when the rotation angle is reduced from $\theta = 3.5^\circ$ to $\theta = 2.0^\circ$. In the CB an ultraflatband is formed and its localization is at the B^{Mo/Mo} region. Such band is almost composed solely by d_0 orbital while it has a finite contribution from p_{xy} orbitals. This indicates a different origin of the ultraflatbands near the conduction band. The electronic states at the conduction band edge are nearly decoupled from each other for two different layers, as there is little interlayer interaction for the B^{Mo/Mo} stacking. This property might allow independent manipulation of electronic states in conduction band minimum for the two different layers.

Conclusions.—We have studied the evolution of the

band structure of twisted bilayer MoS₂. We found that as the rotation angle decreases, the band width decreases monotonically and the flatband wave functions become more localized as well. When the rotation angle is below a certain value, flatbands start to emerge at the valence band and multiple energy-separated flatbands form at the conduction band. Furthermore, compression and mechanical strain are effective methods to tune the flatbands and their localization in real space. Finally, we analyzed the orbital composition near the band edge in the presence of SOC. We show that, while SOC in the valence band is suppressed by the Moiré interaction and nearly restored inversion symmetry, in the conduction band edge the states are spin-polarized. Moreover, the polarization is opposite in K and K' . Therefore, the effect of spin-orbit coupling should be taking into account when developing simpler models for this kind of systems. We also found that the electronic states at conduction band edge are independent for the two layers according to their orbital contribution. All these interesting properties are also occur in other twisted bilayer TMDCs, for instance, MoSe₂, WS₂ and WSe₂, which indicates that twisted TMDCs could be used as an ideal platform for the understanding of correlated behaviors.

Acknowledgments—This work was supported by the National Science Foundation of China under Grant No. 11774269. G Yu acknowledges a support from the China Postdoctoral Science Foundation (Grant No. 2018M632902). Numerical calculations presented in this paper have been performed on the supercomputing system in the Supercomputing Center of Wuhan University.

* josilgui@gmail.com

† s.yuan@whu.edu.cn

- [1] R. Bistritzer and A. H. MacDonald, Moiré bands in twisted double-layer graphene, *Proceedings of the National Academy of Sciences* **108**, 12233 (2011).
- [2] I. Brihuega, P. Mallet, H. González-Herrero, G. T. De Laissardière, M. Ugeda, L. Magaud, J. Gómez-Rodríguez, F. Ynduráin, and J.-Y. Veuillen, Unraveling the intrinsic and robust nature of van hove singularities in twisted bilayer graphene by scanning tunneling microscopy and theoretical analysis, *Physical review letters* **109**, 196802 (2012).
- [3] Y. Cao, V. Fatemi, A. Demir, S. Fang, S. L. Tomarken, J. Y. Luo, J. D. Sanchez-Yamagishi, K. Watanabe, T. Taniguchi, E. Kaxiras, *et al.*, Correlated insulator behaviour at half-filling in magic-angle graphene superlattices, *Nature* **556**, 80 (2018).
- [4] Y. Cao, V. Fatemi, S. Fang, K. Watanabe, T. Taniguchi, E. Kaxiras, and P. Jarillo-Herrero, Unconventional superconductivity in magic-angle graphene superlattices, *Nature* **556**, 43 (2018).
- [5] A. Kerelsky, L. J. McGilly, D. M. Kennes, L. Xian, M. Yankowitz, S. Chen, K. Watanabe, T. Taniguchi, J. Hone, C. Dean, *et al.*, Maximized electron interactions at the magic angle in twisted bilayer graphene, *Nature* **572**, 95 (2019).
- [6] Y. Xie, B. Lian, B. Jäck, X. Liu, C.-L. Chiu, K. Watanabe, T. Taniguchi, B. A. Bernevig, and A. Yazdani, Spectroscopic signatures of many-body correlations in magic-angle twisted bilayer graphene, *Nature* **572**, 101 (2019).
- [7] T. Wolf, J. L. Lado, G. Blatter, and O. Zilberberg, Electrically tunable flat bands and magnetism in twisted bilayer graphene, *Physical review letters* **123**, 096802 (2019).
- [8] F. Wu, T. Lovorn, E. Tutuc, and A. H. MacDonald, Hubbard model physics in transition metal dichalcogenide moiré bands, *Physical review letters* **121**, 026402 (2018).
- [9] M. H. Naik and M. Jain, Ultraflatbands and shear solitons in moiré patterns of twisted bilayer transition metal dichalcogenides, *Physical review letters* **121**, 266401 (2018).
- [10] M. H. Naik, S. Kundu, I. Maity, and M. Jain, Origin and evolution of ultraflatbands in twisted bilayer transition metal dichalcogenides: Realization of triangular quantum dots, *arXiv preprint arXiv:1908.10399* (2019).
- [11] M. Fleischmann, R. Gupta, S. Sharma, and S. Shallcross, Moiré quantum well states in tiny angle two dimensional semi-conductors, *arXiv preprint arXiv:1901.04679* (2019).
- [12] Z. Zhang, Y. Wang, K. Watanabe, T. Taniguchi, K. Ueno, E. Tutuc, and B. J. LeRoy, Flat bands in small angle twisted bilayer WSe₂, *arXiv preprint arXiv:1910.13068* (2019).
- [13] L. Wang, E.-M. Shih, A. Ghiotto, L. Xian, D. A. Rhodes, C. Tan, M. Claassen, D. M. Kennes, Y. Bai, B. Kim, K. Watanabe, T. Taniguchi, X. Zhu, J. Honebio, A. Pasupathy, and C. R. Dean, Magic continuum in twisted bilayer WSe₂, *arXiv preprint arXiv:1910.12147* (2019).
- [14] F. Wu, T. Lovorn, E. Tutuc, I. Martin, and A. H. MacDonald, Topological insulators in twisted transition metal dichalcogenide homobilayers, *Physical review letters* **122**, 086402 (2019).
- [15] J. Wang, Q. Shi, E.-M. Shih, L. Zhou, W. Wu, Y. Bai, D. A. Rhodes, K. Barmak, J. Hone, C. R. Dean, and X.-Y. Zhu, Excitonic phase transitions in MoSe₂/WSe₂ heterobilayers, *arXiv preprint arXiv:2001.03812* (2020).
- [16] C. Jin, E. C. Regan, A. Yan, M. I. B. Utama, D. Wang, S. Zhao, Y. Qin, S. Yang, Z. Zhang, S. Shi, K. Watanabe, T. Taniguchi, S. Tongay, A. Zettl, and F. Wang, Observation of moiré excitons in WSe₂/WS₂ heterostructure superlattices, *Nature* **567**, 76 (2019).
- [17] E. C. Regan, D. Wang, C. Jin, M. I. B. Utama, B. Gao, X. Wei, S. Zhao, W. Zhao, Z. Zhang, K. Yumigeta, M. Blei, J. D. Carlström, K. Watanabe, T. Taniguchi, S. Tongay, M. Crommie, A. Zettl, and F. Wang, Mott and generalized wigner crystal states in WSe₂/WS₂ moiré superlattices, *Nature* **579**, 359 (2020).
- [18] Y. Shimazaki, I. Schwartz, K. Watanabe, T. Taniguchi, M. Kroner, and A. Imamoğlu, Moiré superlattice in a MoSe₂/hBN/MoSe₂ heterostructure: from coherent coupling of inter-and intra-layer excitons to correlated mott-like states of electrons, *arXiv preprint arXiv:1910.13322* (2019).
- [19] J. Sung, Y. Zhou, G. Scuri, V. Zólyomi, T. I. Andersen, H. Yoo, D. S. Wild, A. Y. Joe, R. J. Gelly, H. Heo, D. Bérubé, A. M. M. Valdivia, T. Taniguchi, K. Watan-

- abe, M. D. Lukin, P. Kim, V. I. Fal'ko, and H. Park, Broken mirror symmetry in excitonic response of reconstructed domains in twisted MoSe₂/MoSe₂ bilayers, arXiv preprint arXiv:2001.01157 (2020).
- [20] Y. Tang, L. Li, T. Li, Y. Xu, S. Liu, K. Barmak, Katayun and Watanabe, T. Taniguchi, A. H. MacDonald, S. Jie, and K. F. Mak, Simulation of hubbard model physics in WSe₂/WS₂ moiré superlattices, *Nature* **579**, 353 (2020).
- [21] Y. Zhang, N. F. Yuan, and L. Fu, Moiré quantum chemistry: charge transfer in transition metal dichalcogenide superlattices, arXiv preprint arXiv:1910.14061 (2019).
- [22] K. Slagle and L. Fu, Charge transfer excitations, pair density waves, and superconductivity in moiré materials, arXiv preprint arXiv:2003.13690 (2020).
- [23] R. Roldán, L. Chirolli, E. Prada, J. A. Silva-Guillén, P. San-Jose, and F. Guinea, Theory of 2D crystals: graphene and beyond, *Chemical Society Reviews* **46**, 4387 (2017).
- [24] B. Amorim, A. Cortijo, F. De Juan, A. Grushin, F. Guinea, A. Gutiérrez-Rubio, H. Ochoa, V. Parente, R. Roldán, P. San-Jose, *et al.*, Novel effects of strains in graphene and other two dimensional materials, *Physics Reports* **617**, 1 (2016).
- [25] S. Carr, S. Fang, P. Jarillo-Herrero, and E. Kaxiras, Pressure dependence of the magic twist angle in graphene superlattices, *Physical Review B* **98**, 085144 (2018).
- [26] L. Chirolli, E. Prada, F. Guinea, R. Roldán, and P. San-Jose, Strain-induced bound states in transition-metal dichalcogenide bubbles, *2D Materials* **6**, 025010 (2019).
- [27] M. A. Cazalilla, H. Ochoa, and F. Guinea, Quantum spin hall effect in two-dimensional crystals of transition-metal dichalcogenides, *Physical review letters* **113**, 077201 (2014).
- [28] C. Zhang, C.-P. Chuu, X. Ren, M.-Y. Li, L.-J. Li, C. Jin, M.-Y. Chou, and C.-K. Shih, Interlayer couplings, moiré patterns, and 2d electronic superlattices in MoS₂/WSe₂ hetero-bilayers, *Science advances* **3**, e1601459 (2017).
- [29] K. Liu, L. Zhang, T. Cao, C. Jin, D. Qiu, Q. Zhou, A. Zettl, P. Yang, S. G. Louie, and F. Wang, Evolution of interlayer coupling in twisted molybdenum disulfide bilayers, *Nature communications* **5**, 1 (2014).
- [30] A. A. Puzdov, L. Liang, X. Li, K. Xiao, B. G. Sumpter, V. Meunier, and D. B. Geohegan, Twisted MoSe₂ bilayers with variable local stacking and interlayer coupling revealed by low-frequency raman spectroscopy, *ACS nano* **10**, 2736 (2016).
- [31] S. Fang, R. K. Deho, S. N. Shirodkar, S. Lieu, G. A. Tritsarolis, and E. Kaxiras, Ab initio tight-binding hamiltonian for transition metal dichalcogenides, *Physical Review B* **92**, 205108 (2015).
- [32] Y. Zhang, Z. Zhan, F. Guinea, J. Á. Silva-Guillén, and Y. Shengjun, Tuning band gaps in twisted bilayer MoS₂, Unpublished.
- [33] R. Roldán, M. P. López-Sancho, F. Guinea, E. Cappelluti, J. Á. Silva-Guillén, and P. Ordejón, Momentum dependence of spin-orbit interaction effects in single-layer and multi-layer transition metal dichalcogenides, *2D Materials* **1**, 034003 (2014).
- [34] H. Shi, Z. Zhan, Z. Qi, K. Huang, E. van Veen, J. Á. Silva-Guillén, R. Zhang, P. Li, K. Xie, H. Ji, *et al.*, Large-area, periodic, and tunable intrinsic pseudo-magnetic fields in low-angle twisted bilayer graphene, *Nature Communications* **11**, 1 (2020).
- [35] E. Cappelluti, R. Roldán, J. Silva-Guillén, P. Ordejón, and F. Guinea, Tight-binding model and direct-gap/indirect-gap transition in single-layer and multilayer MoS₂, *Physical Review B* **88**, 075409 (2013).
- [36] See Supplementary Materials for details regarding the localization of the wave functions of the ultraflatbands, the charge density, the effect of the local deformation, the effect of the spin-orbit coupling, the band structure of MoSe₂, WS₂ and WSe₂, the effect of the lattice relaxation and the computational details, .
- [37] H. Huang and F. Liu, Comparison of quantum spin hall states in quasicrystals and crystals, *Physical Review B* **100**, 085119 (2019).
- [38] N. Bandaru, R. S. Kumar, D. Sneed, O. Tschauner, J. Baker, D. Antonio, S.-N. Luo, T. Hartmann, Y. Zhao, and R. Venkat, Effect of pressure and temperature on structural stability of MoS₂, *The Journal of Physical Chemistry C* **118**, 3230 (2014).
- [39] F. Guinea, M. Katsnelson, and A. Geim, Energy gaps and a zero-field quantum hall effect in graphene by strain engineering, *Nature Physics* **6**, 30 (2010).
- [40] A. Branny, S. Kumar, R. Proux, and B. D. Gerardot, Deterministic strain-induced arrays of quantum emitters in a two-dimensional semiconductor, *Nature communications* **8**, 1 (2017).
- [41] A. Reserbat-Plantey, D. Kalita, Z. Han, L. Ferlazzo, S. Autier-Laurent, K. Komatsu, C. Li, R. Weil, A. Ralko, L. Marty, *et al.*, Strain superlattices and macroscale suspension of graphene induced by corrugated substrates, *Nano letters* **14**, 5044 (2014).
- [42] H. Li, A. W. Contryman, X. Qian, S. M. Ardakani, Y. Gong, X. Wang, J. M. Weisse, C. H. Lee, J. Zhao, P. M. Ajayan, *et al.*, Optoelectronic crystal of artificial atoms in strain-textured molybdenum disulfide, *Nature communications* **6**, 1 (2015).
- [43] Y. Liu, J. Rodrigues, Y. Z. Luo, L. Li, A. Carvalho, M. Yang, E. Laksono, J. Lu, Y. Bao, H. Xu, *et al.*, Tailoring sample-wide pseudo-magnetic fields on a graphene-black phosphorus heterostructure, *Nature nanotechnology* **13**, 828 (2018).
- [44] H. Ochoa and R. Roldán, Spin-orbit-mediated spin relaxation in monolayer MoS₂, *Physical Review B* **87**, 245421 (2013).